Production of High Purity MnSO<inf>4</inf>·H<inf>2</inf>O from Real NMC111 Lithium-Ion Batteries Leachate Using Solvent Extraction and

(article starts on next page)

Production of High Purity MnSO$_4$·H$_2$O from Real NMC111 Lithium-Ion Batteries Leachate Using Solvent Extraction and Evaporative Crystallization

Andrea Locati, Maja Mikulić, Léa M.J. Rouquette, Burçak Ebin & Martina Petranikova

View supplementary material

Published online: 04 Dec 2024.

Submit your article to this journal

Article views: 101

View related articles

View Crossmark data

Production of High Purity MnSO$_4$·H$_2$O from Real NMC111 Lithium-Ion Batteries Leachate Using Solvent Extraction and Evaporative Crystallization

Andrea Locati [ID], Maja Mikulić, Léa M.J. Rouquette [ID], Burçak Ebin [ID], and Martina Petranikova [ID]

Department of Chemistry and Chemical Engineering, Industrial Materials Recycling and Nuclear Chemistry, Chalmers University of Technology, Chalmers University of Technology, Gothenburg, Sweden

ABSTRACT

Recovery of manganese as high purity MnSO$_4$·H$_2$O from purified NMC111 lithium-ion battery leachate using solvent extraction and evaporative crystallization was investigated. Bis(2-ethyl-hexyl) phosphoric acid (D2EHPA) was used for Mn extraction. Operational parameters for extraction, scrubbing, and stripping (e.g. pH, number of stages, phases composition) were determined based on the results of batch equilibrium experiments. Counter-current extraction in bench-scale mixer settlers (V$_{MSU}$=120 mL) was carried out with 35% v/v (1.05 M) D2EHPA in Isopar L operated at an average pH of 2.9 and θ = 1. More than 98% of the Mn was extracted in three counter-current stages together with 4%, 5% and 3% of Co, Li and Ni respectively. The distribution of impurities such as Zn, Ca, and Al was monitored during counter-current operations. Satisfactory removal of Co, Ni and Li from the loaded organic phase was achieved after contact with a solution of Mn 4 g/L (70 mM) in two stages at θ = 1. A solution with a Mn concentration of 8.7 g/L (160 mM) was recovered after stripping with 0.5 M H$_2$SO$_4$ at θ = 1 in two stages. Evaporative crystallization of the product allowed the recovery of high purity (99.6%) MnSO$_4$·H$_2$O. A flowsheet for Mn recovery from LIBs is proposed, and the advantages and challenges related to it are discussed.

Introduction

The increased awareness of the need for enhancing sustainability for reducing climate change led to an intensification of electrification in many sectors.[1] Among such, the electrification of transportation is expected to be the main driver of a global increase in the demand for lithium-ion batteries (LIBs) in the next decade.[2] According to the McKinsey Battery Insights study carried out in 2022, the value of the entire LIBs value chain is expected to grow by over 30%

annually, exceeding the value of 400 billion in 2030 with a market size of 4.7 TWh (1 Battery pack = 8–100 kWh, 150–600 kg[3]).[1] The need of fulfilling the intensified LIBs demand by granting a steady supply of both raw materials and equipment, together with the status of critical raw materials associated to many elements nowadays employed in the production of LIBs (e.g., Co, Li, Mn, and Ni[4]), led to the development of new regulations (e.g., European Battery Regulation, 2023[5]) to drive in the development of efficient and reliable recycling processes.[1,6]

Nowadays, the LIBs market is dominated by lithium nickel manganese cobalt oxide ($LiNi_xMn_yCo_{1-x-y}O_2$, NMC) and lithium iron phosphate ($LiFePO_4$, LFP) cathode chemistries, which accounted for 42% and 47% of the global demand in 2022.[2] Many of the recycling processes developed focus on NMC LIBs, due to the high value of the metals that compose the cathode material. A set of hydrometallurgical, pyrometallurgical, or combined routes have been proposed, and several reviews summarizing available information have been published.[3,6,7] Among these, the hydrometallurgical approach has been recently widely investigated since it allows to achieve high recovery rates and high purity of the final products, together with reduced energy consumption and modest greenhouse gases (GHG) emissions. However, upstream sorting of batteries by chemistry is required and the efficiency of mechanical pre-treatment plays a decisive role in determining the quality of the products.[3,6–8]

The first step in the hydrometallurgical recycling route is the leaching of the black mass, a mixture of cathode, and anode active materials obtained after the pre-treatment stages. The most widely used reagents are mineral acids (e.g., H_2SO_4, HCl, and HNO_3) to which some reducing agents (e.g., H_2O_2) can be added to reduce the transition metals present in the cathode, improving their leachability (e.g. $Co^{3+} \rightarrow Co^{2+}$).[9] Among the mineral acids, sulfuric acid is the most widely used due to its cost, effectiveness, and compatibility with the downstream separation operations.[3,6,7] The solution produced is referred to as pregnant leach solution (PLS) and contains Li, Mn, Co, and Ni together with some Al, Fe, and Cu which are treated as impurities and removed using precipitation, solvent extraction (SX) or ion-exchange (IX).[10–12] The purified PLS can be processed to obtain Li, Mn, Co, and Ni in a chemical form that can be used as cathode material precursors.[3,6,13]

Approaches exploiting different unit operations can be used for the separation and recovery of such metals.[3] Separation of Mn, Co, Ni, and Li by solvent extraction allows high separation efficiencies and high recovery rates with processes that can be operated close to ambient temperature and can process large volumes of solutions in short times due to the fast kinetics of commercially available extractants.[14] Due to the selectivity of the available extractants (e.g., D2EHPA, Cyanex 272), Mn is commonly the first extracted transition metals in SX processes

applied for LIBs recycling.[15] Avoiding Mn contamination of the Co and Ni products has been the main driver for Mn recovery from LIBs in the past. However, in 2023 the European Union added Mn to the list of critical raw materials due to an increase in its supply risk.[4] Most of the available Mn is indeed mined outside Europe. In 2021, 19.16 Mmt (million metric tons) were mined in South Africa, 7.00 Mmt in Gabon, and 6.95 Mmt in China.[16] Moreover, most of the refining is carried out in China, which also has a dominant role in the production of high-purity manganese, the material of interest for production of LIBs cathode active material.[16,17] Therefore, despite the low share of Mn which is globally devoted to the LIBs market (1% compared to 80–90% used for steelmaking[18,19]), its recovery could help lower the risks associated with its supply and fulfil the recycling goals set by the new European regulation.

Investigation of the use of SX for recovery of Mn upstream of Co/Ni separation and Li recovery has been reported in literature.[6,14,15,20–24] Bis (2-ethylhexyl) phosphoric acid (D2EHPA) has previously been investigated for the extraction of Mn from spent LIBs purified PLS.[15,20,21,23,25] *Vieceli et al.*[15] report a single-stage efficiency higher than 70% for Mn from a simulated LIBs leachate when 0.5 M D2EHPA in Isopar L is used at pH equal to 3.25. The same author[20] proposed a flowsheet for recovery of MnO_2 from LIBs leachate in chloride media using two extraction stages at pH equal to 2.5, one scrubbing stage, and one stripping stage. *Jantunen et al.*[14] achieved extraction of 94.2% Mn by 0.8 M D2EHPA from simulated LIBs leachate in three counter current stages at pH 2.1–2.5.

Downstream solvent extraction process, high-purity Mn can be recovered in different forms (e.g., oxide or sulfate salt) to be utilized as a cathode active material precursor. Methods such as coprecipitation and spray pyrolysis are commercialized and industrially employed for cathode active material production.[26] The main criteria for the choice of the source of transition metals for cathode synthesis in wet chemistry method are the type of solvent and the solubility of the salts used as precursors. Despite the source of transition metals does not seem to play a major role in determining the performances of the newly synthetized cathode active material, for methods which use deionized water, metal sulfate hydrate salts emerged as the most common choice due to their availability on the market.[26] Production of such metal salts by evaporative crystallization (EC) of the SX aqueous product is indicated to be common practice due to the maturity of the technique and the possibility of achieving high crystal growth rates.[13]

The purpose of this work is to investigate the production of $MnSO_4 \cdot H_2O$ from real (industrially pre-treated) NMC111 LIBs purified PLS by solvent extraction and evaporative crystallization. Furthermore, another objective was to observe

the behaviour of impurities during counter current operations since their presence has a crucial impact on the purity of recovered salt.

Materials and methods

Chemicals

Spent EV battery modules were provided by Volvo Cars AB, Sweden. Dismantling and discharging were carried out by STENA Recycling AB, Sweden. Battery cells (750 kg) were crushed and underwent mechanical separation at Akkuser Oy, Finland. The black mass coming from the crushing process was leached with 2 M H_2SO_4, solid-to-liquid ratio 200 g/L at 50°C. Leaching conditions were developed by Aalto University, Finland; while both the leaching process and the removal of Fe, Al and Cu were carried out by Metso, Finland. Shortly, Cu was removed by precipitation of CuS through the addition of a stoichiometric amount of gaseous H_2S at 50°C. Al and Fe were selectively precipitated by addition of NaOH and H_2O_2 at temperatures between 50°C and 80°C. The composition of the feed solution can be found in Table 1. The ionic strength of the solution was 6.5 M, the pH was 5.2 ± 0.1, and the redox potential was 235 mV.

The organic phase used for the solvent extraction experiments was prepared by dissolving Bis(2-ethylhexyl) phosphoric acid (D2EHPA, 97%, Sigma Aldrich, Germany) in Isopar L (Exxon Mobil, USA). The extractant was used without further purification. NaOH solutions were produced by dissolving NaOH pellets (>99%, EMSURE) in Milli-Q water and used for pH control together with concentrated H_2SO_4 (95–98%, Sigma Aldrich, Germany). The same sulfuric acid solution was diluted in Milli-Q water to prepare the solution used for stripping of the loaded organic, whereas $MnSO_4·H_2O$ (>99%, Sigma Aldrich, Germany) was dissolved in Milli-Q water to prepare the phase used for scrubbing.

Batch experiments

Batch experiments for Mn extraction were carried out in 100 mL PP vessels contacting a total volume of about 30 mL. Phases were mixed at about 1000 rpm for 15 min using a mixer from the mixer settler's unit. pH

Table 1. Composition of the purified feed solution. Values for which uncertainty is reported are an average of five ICP-OES measurements. Fe, Cu, and Cd were <LOQ (approximately 0.5, 1 and 0.3 mg/L respectively). F^-, Cl^-, and NO_3^- were measured by ion-chromatography. NO_3^- was <LOD(5 mg/L).

	Li	Ni	Co	Mn	Na	SO_4^{2-}	F^-
c (g/L)	4.16 ± 0.09	6.7 ± 0.2	11.2 ± 0.3	10.1 ± 0.2	57.5 ± 1.4	60.3 ± 1.5	0.1
c (mM)	600 ± 10	115 ± 3	190 ± 4	185 ± 4	2480 ± 60	1879 ± 48	5.6
	Al	Zn	Si	Mg	Ca	P	Cl^-
c (mg/L)	34 ± 4	2 ± 1	8 ± 1	11 ± 1	15 ± 5	43 ± 4	25

adjustment was performed by addition of 10 M NaOH or concentrated H_2SO_4 solutions. Sampling was performed after satisfactory phase separation was visually observed. For determining scrubbing and stripping conditions, when no control of the equilibrium pH was required, the experiments were carried out in glass vials (3.5 mL) using a shaking machine (IKA-Vibrax, Germany) at 1500 rpm for 20 min. Samples were centrifuged at 5000 rpm for 5 min to guarantee satisfactory phase separation. In both cases, temperature was kept constant at 25 ± 1°C by using an external thermostat.

Counter current experiments

Continuous counter current experiments were carried out in MEAB Mixer-settler units (MEAB Metalextraktion AB, Sweden). The active volumes of mixer and settler were estimated to be 40 and 80 mL, respectively. The aqueous feed and the organic phase were fed using electromagnetic pumps (EW-B08TC-20EPF2, EWN-B11TCER, IWAKI, Japan) with a flow rate of about 5 mL/min each (τ_{mix} = 4 min, θ = 1). Mixing at about 1000 rpm was performed. The pH was controlled by feeding 10 M NaOH in the mixing chamber of each stage using peristaltic pumps (BT103S, Lead Fluid, China). The counter current extraction, scrubbing, and stripping experiments were carried out separately to allow testing for the subsequent stage on the real solution. For instance, after counter current extraction, scrub batch experiments were performed on the produced loaded organic. All the continuous counter current experiments were performed at room temperature (23 ± 2°C). A picture of the counter-current extraction stages is available in the supplementary material (Figure S1).

Evaporative crystallization

Crystallization of $MnSO_4 \cdot H_2O$ from the produced stripping solution was performed in a rotary evaporator (RE150–220, Labfirst Scientific, China), at 50°C and 50 mbar. The obtained crystals were washed multiple times with ethanol (95%) to remove traces of liquid residues and dried at 50°C before analysis.

Analytical methods

Metal concentration in liquid samples was analyzed with ICP-OES (Thermo Fisher Scientific, iCAP™ 6000 Series, USA). The concentration of F^- in the feed was measured by ion chromatography while an ion selective electrode was used to measure its concentration in the stripping product. The concentration of NO_3^- and Cl^- in the feed and stripping product was measured by ion chromatography.

To measure the concentration of metals in the organic phase, back extraction of the loaded organic with 5 M H_2SO_4 at A:O = 5 was performed, and the H_2SO_4 raffinates were analysed. ICP-MS (Thermo Fisher Scientific, iCAP Q), was used to determine the content of impurities in the produced Mn salt. Further characterization of the solid samples was performed using X-ray diffraction analysis (XRD, Bruker D8 Discover) using a Cu source with wavelength 1.5406 Å, 2θ between 10° and 80°, 15 rpm rotation speed, and generator settings of 40 mA and 40 kV. EVA software (Bruker AXS – DIFFRAC.EVA.Version 6.0) and JCPDS database (International Centre for Diffraction Data, ICDD, PDF-5+) were used for analytical interpretation. Scanning Electron Microscopy coupled with Energy Dispersive X-ray Spectroscopy (SEM-EDS, FEI Quanta 100 FEG SEM with an Oxford Instruments X-Max EDS detector) was used to investigate the morphology of the solid samples and validate the elemental composition of the salts analysed by ICP techniques.

The pH of the aqueous phases was measured using a pH electrode (Metrohm 827 pH lab, Metrohm 6.0234.100, Switzerland) calibrated with pH buffers 2, 4, and 7 (Merck, Germany). The redox potential was measured with an ORP electrode (Metrohm 6.0451.100, Switzerland) connected to the 905 Titrando unit (Metrohm, Switzerland). Before use, the electrode was tested with a reference $HgCl_2$ solution of 250 mV (Merck, Germany).

Data treatment

The distribution ratio (D) of the metals was computed using Equation (1).

$$D = \frac{[\bar{M}]_{tot}}{[M]_{tot}} = \frac{[M]_0 - [M]}{[M]} \tag{1}$$

Where M denotes a generic metal and the overbar indicates that the species is in the organic phase. The subscript "0" indicates the initial concentration of the metal, otherwise the equilibrium concentrations must be intended.

The percentage of extraction was calculated using Equation (2).

$$\%E = \frac{100 \cdot D}{D + 1/\theta} = \frac{[M]_0 - [M]}{[M]_0} \tag{2}$$

Where θ also indicated as O:A, is the ratio between the volume of the organic phase (V_{org}) and the volume of the aqueous phase (V_{aq}) and is sometimes referred to as "phase ratio" in the following text.

The purity of the produced salt was assessed using Equation (3).

$$P_{R,M} = 100 \cdot \frac{w_M}{\sum_i w_i} \tag{3}$$

Where $P_{R,M}$ is the relative purity of the metal M [wt.%], w is either the weight concentration [g L^{-1}] or the weight fraction [g_{metal} g_{sample}^{-1}] depending on if the purity of a liquid solution or of a solid is stated, and i is an index that refers to all the considered metals. Despite being the most used method for purity calculations, using weight concentrations/fractions provides results which neglect the differences in the molar mass of the elements. Values of purity of the products computed using molarity [mol L^{-1}] and moles content in a certain mass of sample [mol_{metal} g_{sample}^{-1}] are reported in the supplementary material (Table S1). Discrepancies in the order of 0.1% were observed.

Results and discussion

Extraction

Effect of pH and extractant concentration on Mn, Co, Ni and Li extraction and determination of number of extraction stages

Two different concentrations of D2EHPA in Isopar L were contacted with the feed solution at different equilibrium pH. The extraction of Mn, Co, Ni, and Li shown in Figure 1 confirms that the selectivity of D2EHPA can be exploited to separate Mn from Co, Ni, and Li. Moreover, according to Equation (4), which shows the simplified extraction mechanism characteristic of acidic extractants, increasing the pH of the aqueous phase favours metal extraction.[27] Mn extraction above 60% was achieved at pH about 3 with coextraction of Co, Li, and Ni being, respectively, 3%, 4%, and less than 1% by using D2EHPA 24% v/v (0.7 M) in Isopar L.
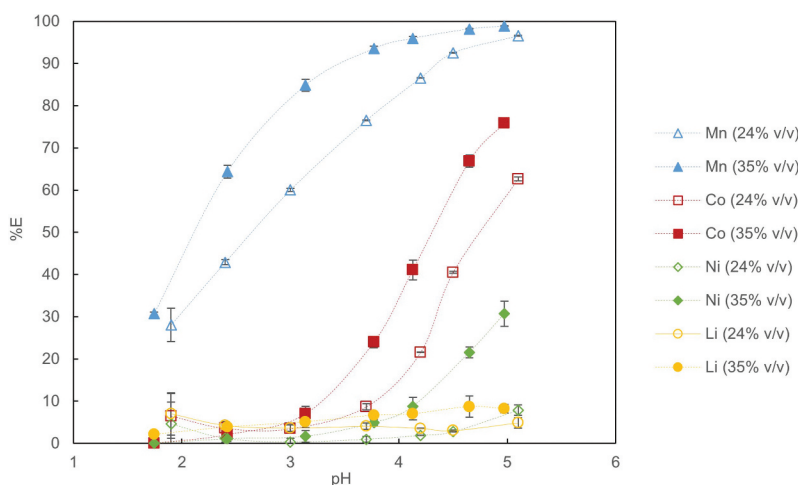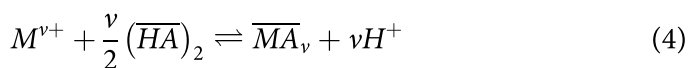

Figure 1. Extraction efficiency as a function of pH for Mn, Co, Ni and Li extracted by D2EHPA in isopar L (concentration is reported in parenthesis). θ = 1, t$_{eq}$=15 min, T = 25 ± 1℃, 1000 rpm. Uncertainties of triplicates are shown. The lines do not represent a fit of the point.

$$M^{v+} + \frac{v}{2}\left(\overline{HA}\right)_2 \rightleftharpoons \overline{MA}_v + vH^+ \tag{4}$$

Increasing the concentration of D2EHPA to 35% v/v (1.05 M) enhanced the extraction of Mn but favoured the coextraction of the other metals as expected by the increased number of free extractant molecules present in the system. Coherently with this, a shift in the pH_{50} was observed. By graphical interpolation, the pH_{50} was estimated to be approximately 2.65 for Mn and 4.76 for Co when the initial concentration of extractant was 0.7 M and decreased to approximately 2.13 for Mn and 4.31 for Co when more concentrated D2EHPA was used. However, good selectivity was achieved at pH around 3.1 with almost 85% of Mn extracted in a single stage and co-extraction of Co, Li, and Ni, respectively, equal to 7%, 5%, and less than 2%. The evolution of the logarithm of the distribution ratio as a function of pH is reported in the supplementary material (Figure S1). Graphical analysis of the McCabe-Thiele diagram shown in Figure 2 suggests that three extraction stages are needed to extract 99.9% of the Mn with $\theta = 1$ at pH = 3.2 ± 0.1 using 35% v/v D2EHPA in Isopar L at $25 \pm 1°C$. The evolution of the extraction of Mn, Co, Ni, and Li as a function of the phase ratio is shown in Figure 3. The results obtained for phase $\theta = 1$ show good agreement with the data obtained in Figure 1 and highlight, as previously observed, that an increase in the number of available extractant molecules enhances the extraction of the metals. The co-extraction of metals other than Co, Ni, and Li was not considered as a criterion in the determination of the conditions for counter-current extraction, due to their low
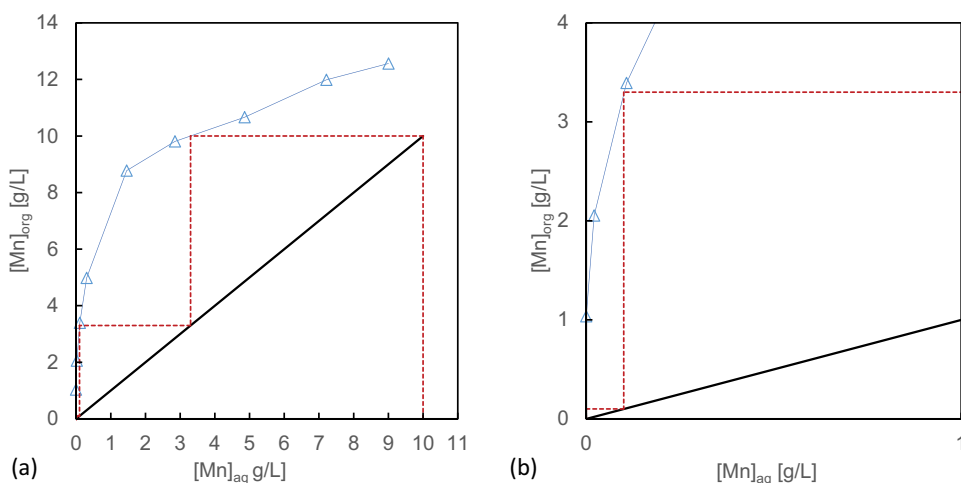

Figure 2. (a) McCabe-Thiele analysis applied to equilibrium distribution of Mn between 35% v/v D2EHPA in isopar L and purified NMC111 feed solution. $T = 25 \pm 1°C$, pH = 3.2 ± 0.1, t_{eq}=15min. Initial $[Mn]_{aq} = 10.1$ g/L (Table 1). (b) Sub-section of the McCabe-Thiele diagram that extends up to $[Mn]_{aq}$=1 g/L and $[Mn]_{org}$=4 g/L. Operating line calculated for extraction of 99.9% of Mn and $\theta = 1$.
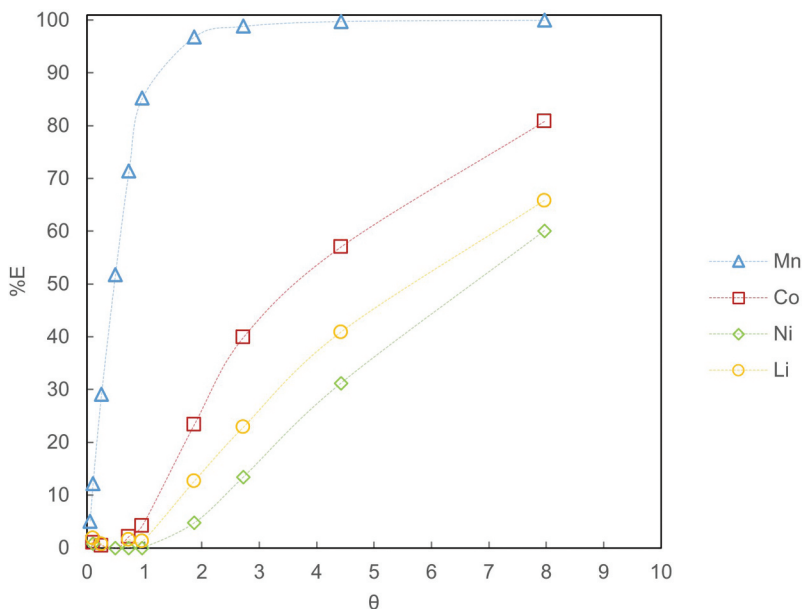
Figure 3. Extraction efficiency of Mn, Co and Li by 35% v/v D2EHPA in isopar L as a function of the phase ratio at pH = 3.2 ± 0.1, t_{eq}=15 min, T = 25 ± 1°C, 1000 rpm.

concentration (Table 1) and to the fact that in industrial processes satisfactory removal of impurities is to be achieved before separation of Mn, Co, Ni, and Li.[14] The distribution of low concentration metals was, however, monitored during counter-current operations.

Counter-current extraction of Mn

Counter-current extraction operations were initially carried out with the aim of achieving pH = 3.2 ± 0.1 in all three stages. However, despite achieving complete Mn extraction with such operational conditions, a significant co-extraction of Co (>15%) was observed. Therefore, the equilibrium pH at which the three stages were operated was lowered and steady state was achieved at pH = 2.9 ± 0.1 in all the stages. According to the conventional theory on residence time distribution steady state was considered achieved after more than five cascade volumes were processed.[28] Another viable option for reducing coextraction is decreasing the flow ratio to increase the crowding of the organic phase. However, to avoid increasing the complexity of the operation of small-scale mixer settlers, no adjustment of the flows of the phases was performed. More than 98% of Mn was extracted in the reported conditions with coextraction of 4%, 5%, and 3% Co, Li, and Ni, respectively. Deviations in the mass balance were estimated to be below 5% by measuring the concentration of metals in the organic phase after stripping with 5 M H_2SO_4 and A:O = 5. Despite reducing the losses of Co due to its coextraction, lowering the operational equilibrium pH

resulted in an incomplete extraction of Mn which would impact the purity of the Co product that is generally produced downstream of Mn extraction.[29]

The evolution of the concentrations of Mn, Co, Ni, and Li in the aqueous and organic phases across the counter-current stages is shown in Figure 4(a). It is evident that Mn is extracted from the aqueous phase, reaching
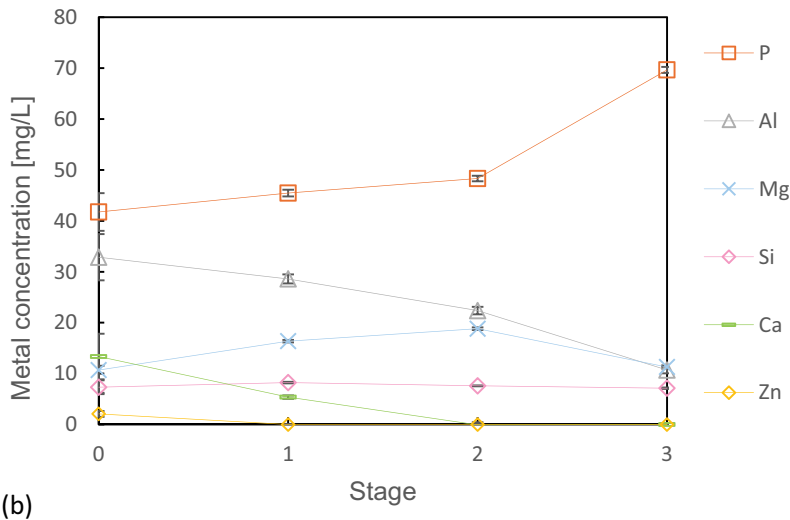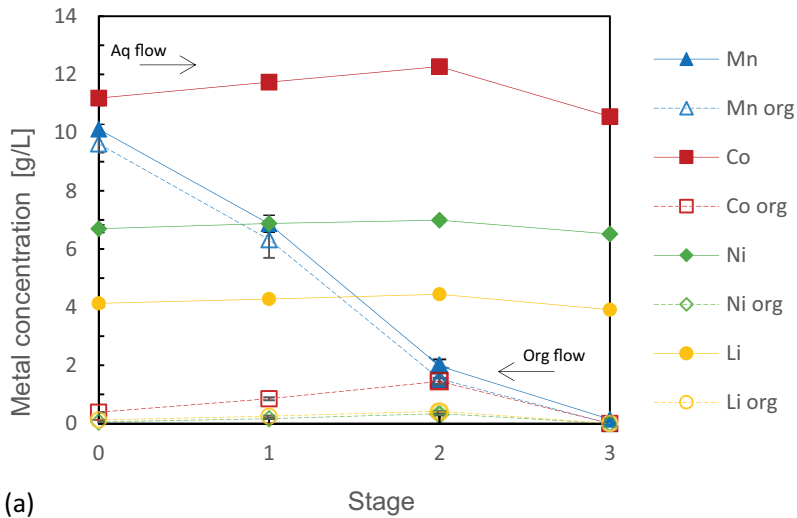

(a)

(b)

Figure 4. (a) Concentrations evolution of Mn, Co, Ni and Li in the aqueous and organic phases and (b) concentrations of P, Al, Mg, Si, Ca and Zn in the aqueous phase in a mixer-settler system composed of three stages operated in steady state at pH= 2.9 ± 0.1. 35% v/v D2EHPA in isopar L, θ = 1, room temperature (23 ± 2 °C). Concentration of the feed solution is reported in Table 1, the concentrations in the aqueous phase are the average of seven samples taken 30 min apart from each other after achieving steady state. Concentrations in the organic phase are an average of three samples taken 1 h apart from each other. Number of stages follows the flow of aqueous phase (left to right).

a concentration of above 9 g/L (~160 mm) in the loaded organic phase produced. Moreover, a peak of Co, Ni, and Li concentration was observed in the aqueous raffinate of stage two and in the organic feed of the same stage. The evolution of Na could not be shown in the plot since NaOH 10 M was added to the system to control the pH, nevertheless a content of about 250 mg/L (~11 mM) of Na in the loaded organic phase was measured.

The evolution of the concentration in the aqueous phase of the low concentration elements is shown in Figure 4(b). Complete coextraction of Ca and Zn was observed in agreement with the known selectivity of D2EHPA in sulfate systems.[30] Moreover, more than 60% of Al was extracted together with 10% of Si and Mg. On the other hand, the concentration of P in the aqueous phase was observed to increase along the stages, suggesting that the extractant, and eventually some of its impurities, have been dissolved in the aqueous phase. It is indeed known that D2EHPA itself has a solubility in aqueous solutions which depends on the ionic strength, the pH and the temperature.[27,31,32] Moreover, impurities such as alcohols, trialkyl-phosphates, monoalkylphosphorus acids, and polyphosphorus or pyrophosphorous compounds are sometimes present in the commercially available D2EHPA. Among such mono-(2-ethylhexyl)phosphoric acid (M2EHPA), tri-(2-ethylhexyl)phosphate (T2EHP) and 2-ethylhexanol have been reported to be the most common and, in some cases, to have a higher solubility in aqueous solution compared to D2EHPA.[31,33] Another cause of the increased P concentration in the aqueous phase could be entrainment, which could be reduced by optimizing the hydrodynamic of the mixing process.[27]

Scrubbing of impurities

The average content of Mn, Co, Ni, and Li in the loaded organic phase downstream counter-current extraction was, respectively, about 8.7, 0.43, 0.08, and 0.13 g/L (160, 7, 1, and 19 mM). The results differ slightly from what was observed in Figure 4, possible reasons could be fluctuation in the ICP analysis or most likely a variation in the flow rates during operation since the extraction was performed on multiple days. In agreement with what has been previously reported, to obtain high-purity $MnSO_4 \cdot H_2O$ a scrubbing stage is needed to remove the undesired impurities. *Vieceli et al.*[20] and *Peng et al.*[23] report the use of a solution containing 4 g/L (70 mM) of Mn prepared, respectively, using $MnCl_2 \cdot 4 H_2O$ and $MnSO_4 \cdot H_2O$. A solution of 4 g/L Mn (pH = 5.1 ± 0.1) produced dissolving $MnSO_4 \cdot H_2O$ in MilliQ H_2O was tested. To avoid losses of Mn, recirculation of the scrubbing product must be integrated in the process flowsheet by, for instance, reuse in the leaching stage or in the extraction. Moreover, to reduce the impact of the recirculation on the process and the chemical consumption, the use of
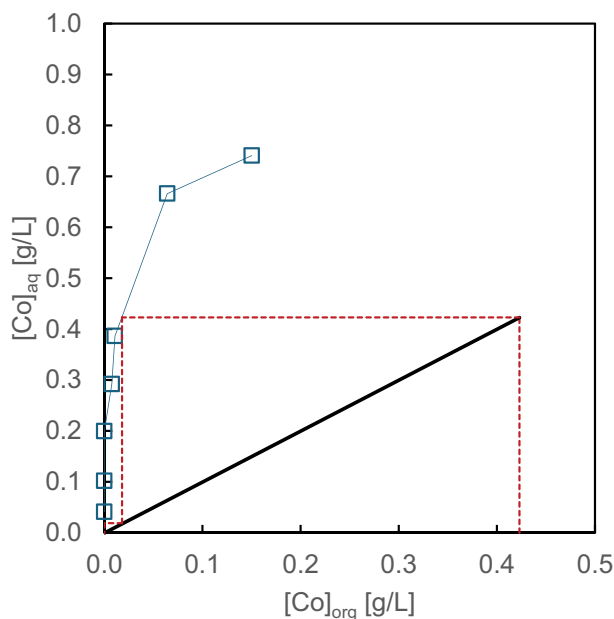
Figure 5. McCabe Thiele diagram for scrubbing of the loaded organic phase after extraction using a solution containing [Mn] = 4 g/L. Initial [Co]$_{org}$ = 430 mg/L. Operating line for 99.9% Co scrubbing at θ=1, T = 25 ± 1°C.

a high θ in the scrubbing operation is desirable.[27] However, in this work, a θ equal to 1 was operated, and no recirculation of the product was tested.

Equation (5) shows the equilibrium that allows the scrubbing of an undesired metal N by contact with an aqueous solution rich in metal M.

$$M^{v+} + \overline{NA_v} \rightleftharpoons \overline{MA_v} + N^{v+} \tag{5}$$
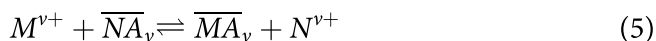
From the results shown in Figure 5, scrubbing of 99.9% of the co-extracted Co can be achieved in two counter-current extraction stages operate at θ equal to 1, using the above reported conditions. Downstream of counter-current operations, an average content of Mn equal to 10.4 g/L (190 mm) was observed in the organic phase, whereas the Co content decreased below 10 mg/l and Li, Ni and Na were below the respective LOQs. Analysis of the aqueous raffinate highlighted the presence of scrubbed Mg, nevertheless no traces of scrubbed Zn and Ca were observed. Moreover, as noticed during operation of the counter-current extraction stages, losses of the extractant in the aqueous stream were highlighted by the higher P concentration of the scrubbing raffinate compared to the feed. The pH of the scrubbing aqueous raffinate was measured to be 2.8 ± 0.1.
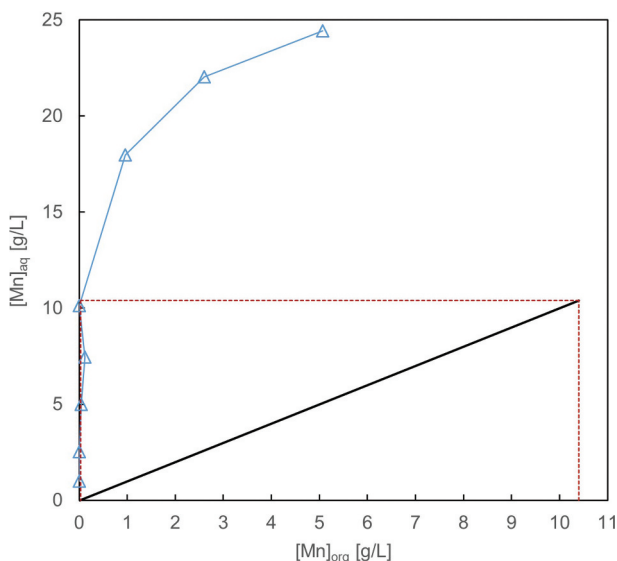
Figure 6. McCabe Thiele diagram for stripping of the loaded organic phase after scrubbing using a solution of 0.5 M H_2SO_4. Input $[Mn]_{org}$ = 10.4 g/L. Operating line for 99.9% Mn stripping at θ=1, T = 25 ± 1°C.

Stripping

The scrubbed organic phase was contacted with a solution of 0.5 M H_2SO_4 to determine the number of stages needed for the stripping operation. The stripping equilibrium can be observed in Equation (4), and the increased proton concentration in the aqueous phase favours the back extraction of the extracted metals by modifying the equilibrium of the system. About 99.9% of the Mn can be stripped in one counter-current stage with a phase ratio equal to one, as shown in Figure 6. However, two counter current stages were operated due to equipment constraints.

The composition of the stripping aqueous product is shown in Table 2 and a relative purity of the final product equal to 99.5 ± 0.5% was predicted.

Approximately 99.5% of the Mn was stripped from the organic phase, which contained on average a residue of 50 mg/L (1 mM) Mn after counter-current operation. The concentration of Mn in the product was measured to be 8.7 g/L

Table 2. Composition of the aqueous stripping solution obtained after operation of the mixer settler units. Li, Si, and Mg were found in traces (<1 mg/L), while Al, Cd, Ni, Fe, and Cu were measured to be below the respective LOQs (0.04, 0.06, 0.1, 0.1, and 0.01 mg/L). Element concentration is reported as an average of three measurements of the aqueous phase. Uncertainty on purity is computed by propagating the uncertainties on concentration of the single elements. Cl^- and NO_3^- were measured by ion-chromatography and were both <LOD(1 mg/L). F^- was measured with an ion selective electrode and were measured to be below LOD (10 mg/L).

	Mn	Co	Na	Zn	Ca	P	Relative Purity
c (mg/L)	8780 ± 30	6 ± 1	1 ± 1	3 ± 1	16 ± 1	14 ± 1	99.5 ± 0.5%

(160 mM), which is lower than what was predicted with mass balance. Fluctuations in the flow rates were indeed noticed during operation and the ratio of the final volumes of stripped organic and product resulted to be lower than one.

Recirculation of a fraction of the final product in the scrubbing stage can be exploited to increase the efficiency of the process in terms of materials use. The differences in Mn content and pH between the synthetic scrubbing solution (pH = 5.1 ± 0.1) and the final product (pH = 0.7 ± 0.1) suggest that further testing is needed to optimize the conditions of the scrubbing operation. Moreover, investigation of the possible reuse of the organic phase and its regeneration should be performed.

Evaporative crystallization of MnSO$_4$.H$_2$O

Evaporative crystallization of MnSO$_4$·H$_2$O was carried out using the product generated by solvent extraction at a temperature of about 50°C and 50 mbar.[13] The product was washed with ethanol, dried at 50°C and manually grinded before analysis. In Figure 7 the sample XRD pattern of the crystals indicates the presence of monohydrated MnSO$_4$ (PDF car no: 04-010-4027). The composition (wt%) of the product is shown in Table 3. A relative purity equal to 99.6 ± 0.1% was computed using Equation (3) according to the ICP analysis results. However, quantification of Fe and Si was not possible by ICP analysis due to matrix interferences. Furthermore, no P was detected when such a technique was used. Weak signals indicating the presence of traces of P and Si (<0.1 wt%) were instead given by SEM-EDS spectra (Figure 8). No measurement of the anionic impurities (F$^-$, NO$_3{}^-$, Cl$^-$) in the salt was performed.

Few information regarding purity requirements for battery grade cathode precursors is available in literature. Moreover, recycling companies do not easily provide data about the requirements of their products. *Nasser et al.*[34] collected values indicating requirements for different battery grade salts, and the data for MnSO$_4$·H$_2$O are included in Table 3. According to such values, the requirements for Mn content in battery grade MnSO$_4$·H$_2$O were fulfilled by the salt produced in the current work, together with the requirements on Cu, Mg, and Cd. On the other hand, the content of Na, Ca, and Zn in the product exceeds the target values. Presence of Ca and Zn in the product was expected due to their coextraction since D2EHPA has been proven to be able to extract both elements at pH lower than Mn. Complete removal of these elements before entering the solvent extraction circuit must be achieved to reduce their presence in the produced Mn salt.[30] Investigation on the effect of some impurities (e.g., Fe, Cu, Al, Ca, and Mg) on the performances of newly synthetized cathode material is available in the literature. Despite the requirements indicated in Table 3, in some cases a beneficial effect due to the presence of impurities was observed.[34–38]
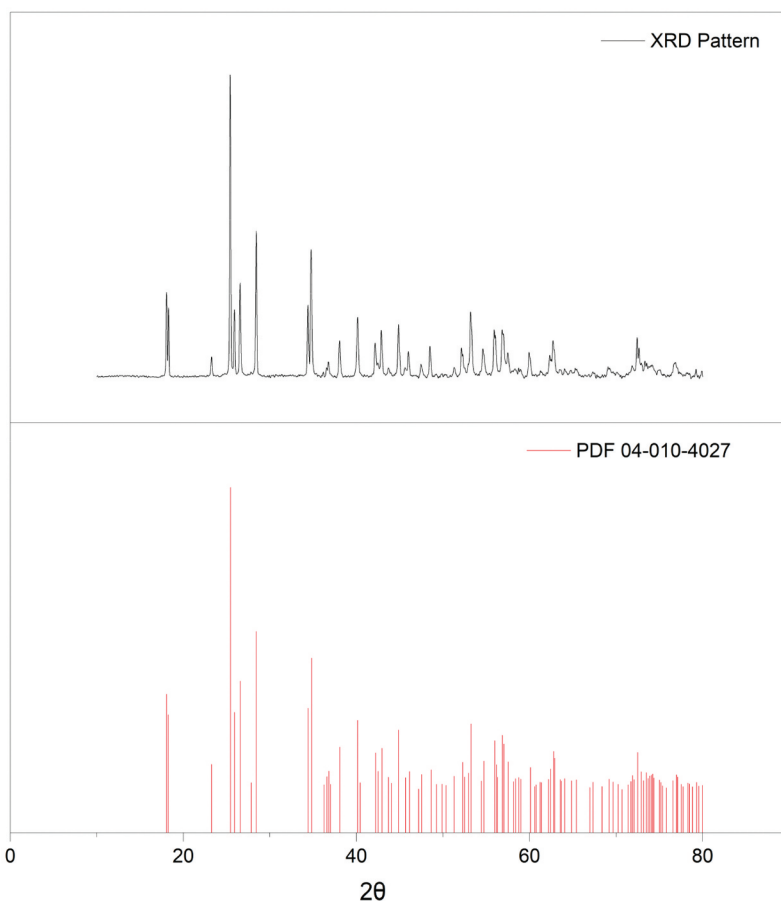
Figure 7. X-ray diffraction pattern of $MnSO_4 \cdot H_2O$ product. Comparison is made with PDF 040-010-4027 for the same compound. Crystalline structure: monoclinic.

Table 3. Comparison between composition (wt%) and purity of the produced $MnSO_4 \cdot H_2O$ and requirements (wt%) for battery grade $MnSO_4 \cdot H_2O$ according to[34] uncertainty of the metals wt% is computed from triplicates. Uncertainty of the purity is obtained by uncertainties propagation.

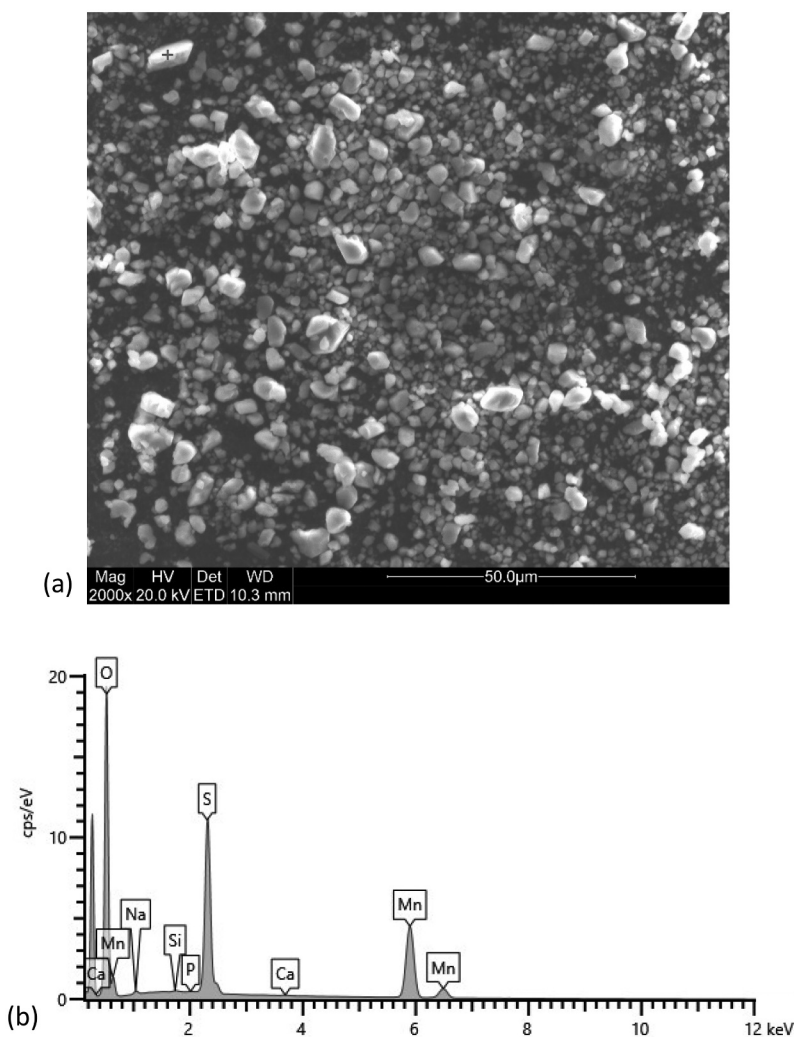|	$MnSO_4.H_2O$ Product (wt%)	Requirements
Mn	32.39 ± 0.03	≥32
Co	0.025 ± 0.001	/
Ni	0.003 ± 0.0001	/
Li	0.001 ± 0.00001	/
Na	0.016 ± 0.006	0.005
Zn	0.010 ± 0.00004	0.001
Mg	0.0021 ± 0.00003	0.005
Ca	0.063 ± 0.002	0.005
Cu	0.0004 ± 0.00002	0.001
Relative Purity	99.6 ± 0.1%	/

Figure 8. SEM picture (a) and EDS spectra (b) of $MnSO_4 \cdot H_2O$ product after ethanol washing, drying, and grinding.

Filtration and subsequent washing of the crystals was necessary due to the presence of a liquid residue in the crystallizer (~80 mL from 3.7 L of starting solution). Analysis of the filtrate highlighted the presence of a high concentration of sulfur (>7 M), residual Mn (3 g/L, 55 mM), and traces of P (100 mg/L, 3 mM). Losses of Mn in the liquid residue below 1% by weight were estimated compared to the expected theoretical mass of salt (99.95 g of $MnSO_4 \cdot H_2O$ from evaporation of 3.7 L of solution).

The presence of highly concentrated sulfur in the filtrate suggests that, during EC operations, water evaporation promoted the concentration of sulfuric acid. A concentration of sulfates of 0.48 mol/L was measured in the stripping product, whereas the total concentration of metals, which can be approximated to be
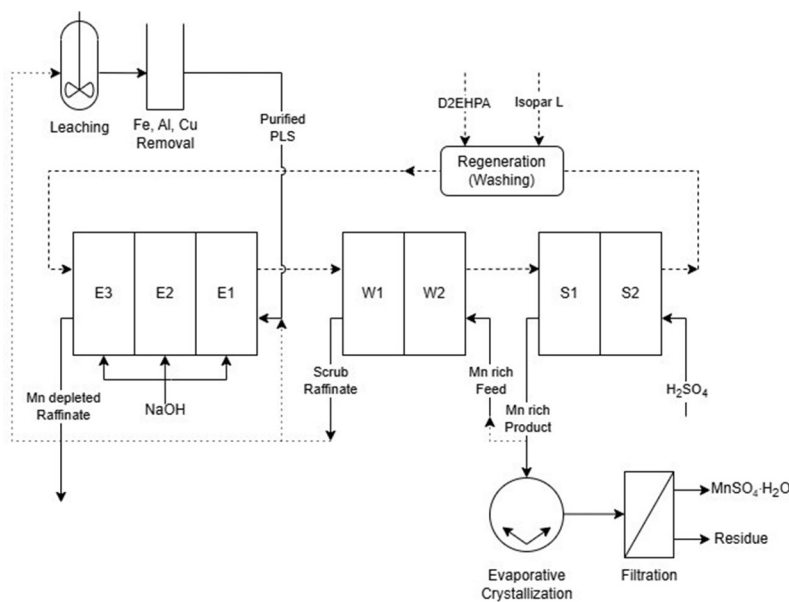
Figure 9. Mn solvent extraction and crystallization flowsheet. Dashed lines represent the flow of organic streams. Dotted lines represent options for streams recirculation.

equal to the concentration of Mn, was found to be 0.16 mol/L. Consequently, since the molar ratio of Mn^{2+} and SO_4^{2-} in the crystals is equal to 1, an excess of 0.32 mol/L of sulfates can be computed. Such excess acid was concentrated up to ~50% by weight in the non-evaporated liquid.

At last, the liquid crystallization residue also contained P coming from the dissolution of D2EHPA and eventually some of its impurities in the aqueous phase, as already discussed in paragraph 3.1.2. Values for the boiling point of D2EHPA, M2EHPA, T2EHP, and 2-ethylhexanol can be found in the literature and are, respectively, 393.4 ± 25.0°C, 320.6 ± 25.0°C (predicted), 215°C, and 184–185°C.[39–42] Such values are all considerably higher than the boiling temperature of water, meaning that if some losses of extractant in the aqueous phase occur, they will contribute to the formation of a liquid residue downstream of evaporative crystallization.

Based on the obtained results, the flowsheet reported in Figure 9 is proposed for Mn extraction from purified NMC111 leachate. If direct production of sulfate salts from the stripping residue of SX is to be performed, minimizing the excess of sulfates in the aqueous phase could be beneficial for minimizing the quantity of liquid by-product generated downstream EC, together with reducing the overall chemical consumption. Moreover, treatment of the stripping residue for removal of the dissolved organic or exploitation of alternative crystallization techniques (e.g., antisolvent crystallization or precipitation) could also be considered.[13,27]

Conclusions

In this study, the feasibility of Mn recovery as a sulfate monohydrate salt from purified NMC111 LIBs PLS by solvent extraction and evaporative crystallization was investigated. Extraction of more than 98% of Mn is achieved in three counter-current stages operated at an average pH of 2.9, with coextraction of Co, Li, and Ni equal to 5%, 4%, and 3% respectively. Two scrubbing stages with a solution of Mn 4 g/L (70 mm) allowed the scrubbing of more than 97% of the co-extracted Co and 99.5% of the Mn present in the loaded organic was stripped after two stages using 0.5 M H_2SO_4. A solution of Mn with a relative purity equal to $99.5 \pm 0.5\%$ was produced and high purity ($99.6 \pm 0.1\%$) $MnSO_4 \cdot H_2O$ was crystallized by evaporative crystallization. Further work is needed to optimize the flowsheet aiming at reducing the chemical consumption, optimizing the flow ratio, reintegrating the scrubbing raffinate into the extraction or leaching stage, and testing the recirculation of the stripping product as a scrubbing agent. Moreover, being solvent extraction a feed-dependent process, careful tuning of the operational parameters should be performed according to the characteristics of the initial aqueous phase. Finally, insights on possible factors which could affect the evaporative crystallization process downstream solvent extraction are reported and could provide some useful data for the future development of LIBs recycling processes.

Disclosure statement

No potential conflict of interest was reported by the author(s).

ORCID

Andrea Locati 🔗 http://orcid.org/0000-0002-9194-9144
Léa M.J. Rouquette 🔗 http://orcid.org/0000-0003-0780-4020
Burçak Ebin 🔗 http://orcid.org/0000-0002-0737-0835
Martina Petranikova 🔗 http://orcid.org/0000-0002-0957-7768

Author's Contribution

Andrea Locati: Data curation, Formal analysis, Investigation, Visualization, Conceptualization, Methodology, Validation, Writing-original draft. Maja Mikulić: Data curation, Formal analysis, Investigation. Léa Rouquette: Analysis support, Writing – review & editing. Burçak Ebin: Supervision, Analysis support, Writing – review & editing. Martina Petranikova: Conceptualization, Methodology, Validation, Writing – review editing, Project administration, Supervision, Funding acquisition.

References

[1] Fleischmann, J.; Hanicke M.; Horetsky E.; Ibrahim D.; Jautelat S.; Linder M.; Schaufuss P.; Torscht L.; van de Rijt A.; Battery 2030: Resilient, Sustainable, and Circular. Battery Demand is Growing — and so is the Need for. *McKinsey & Company*. 2023, [Online]. https://www.mckinsey.com/industries/automotive-and-assembly/our-insights/battery-2030-resilient-sustainable-and-circular#/.

[2] Business Sweden. The Nordic Battery Value Chain, [Online]. https://businitiativeweb sites.blob.core.windows.net/nordics-battery-collaboration/assets/Nordic_Battery_ Report_June_2023_f62fa7ab86.pdf (accessed February, 2023).

[3] Latini, D., Vaccari, M., Lagnoni, M., Orefice, M., Mathieux, F., Huisman, J., Tognotti, L., Bertei, A. A Comprehensive Review and Classification of Unit Operations with Assessment of Outputs Quality in Lithium-Ion Battery Recycling. *J. Power Sources* 2022, *546*. Elsevier B.V., 231979. DOI: 10.1016/j.jpowsour.2022.231979.

[4] European Commission. Study on the Critical Raw Materials for the EU 2023 Final Report, 2023. DOI: 10.2873/725585.

[5] European Commission. Regulation (EU) 2023/1542 of the European Parliament and of the Council Concerning Batteries and Waste Batteries. *Eur. Commission 2023*, *2023* (June), 1–117. [Online]. DOI: http://data.europa.eu/eli/reg/2023/1542/oj%0Ahttps:// eur-lex.europa.eu/legal-content/EN/TXT/?uri=CELEX%3A52020PC0798.

[6] Neumann, J., Petranikova, M.; Meeus, M.; Gamarra, J. D.; Younesi, R.; Winter, M.; Nowak, S. *Recycling of Lithium-Ion Batteries-Current State of the Art, Circular Economy, and Next Generation Recycling*; 2022. DOI: 10.1002/aenm.202102917.

[7] Piątek, J.; Afyon, S.; Budnyak, T. M.; Budnyk, S.; Sipponen, M. H.; Slabon, A. Sustainable Li-Ion Batteries: Chemistry and Recycling. *Adv. Energy Mater.* 2021, *11*(43). DOI: 10. 1002/aenm.202003456.

[8] Gerold, E.; Schinnerl, C.; Antrekowitsch, H. Critical Evaluation of the Potential of Organic Acids for the Environmentally Friendly Recycling of Spent Lithium-Ion Batteries. *Recycling*. 2022, *7*(1). DOI: 10.3390/recycling7010004.

[9] Vieceli, N.; Benjamasutin, P.; Promphan, R.; Hellström, P.; Paulsson, M.; Petranikova, M. Recycling of Lithium-Ion Batteries: Effect of Hydrogen Peroxide and a Dosing Method on the Leaching of LCO, NMC Oxides, and Industrial Black Mass. *ACS*

Sustain. Chem. Eng. 2023, *11*(26), 9662–9673. DOI: 10.1021/ACSSUSCHEMENG. 3C01238.

[10] Virolainen, S.; Wesselborg, T.; Kaukinen, A.; Sainio, T. Removal of Iron, Aluminium, Manganese and Copper from Leach Solutions of Lithium-Ion Battery Waste Using Ion Exchange. *Hydrometallurgy.* 2021, *202*. DOI: 10.1016/j.hydromet.2021.105602.

[11] Nozari, I.; Azizi, A. An Investigation into the Extraction Behavior of Copper from Sulfate Leach Liquor Using Acorga M5640 Extractant: Mechanism, Equilibrium, and Thermodynamics. *Min. Metall. Explor.* 2020, *37*(5), 1673–1680. DOI: 10.1007/s42461-020-00280-z/Published.

[12] Klaehn, J. R.; Shi, M.; Diaz, L. A.; Molina, D. E.; Reich, S. M.; Palasyuk, O.; Repukaiti, R.; Lister, T. E. Removal of Impurity Metals as Phosphates from Lithium-Ion Battery Leachates. *Hydrometallurgy.* 2023, *217*, 106041. DOI: 10.1016/j.hydromet.2023.106041.

[13] Ma, Y.; Svärd, M.; Xiao, X.; Gardner, J. M.; Olsson, R. T.; Forsberg, K. Precipitation and Crystallization Used in the Production of Metal Salts for Li-Ion Battery Materials: A Review. *Met. (Basel).* 2020, *10*(12), 1–16. DOI: 10.3390/met10121609.

[14] Jantunen, T. S. N.; Virolainen, S.; Sainio, T. Direct Production of Ni – Co – Mn Mixtures for Cathode Precursors from Cobalt-Rich Lithium-Ion Battery Leachates by Solvent Extraction. *Met. (Basel).* 2022, *12*(1445), 1445. DOI: 10.3390/met12091445.

[15] Vieceli, N.; Reinhardt, N.; Ekberg, C.; Petranikova, M. Optimization of Manganese Recovery from a Solution Based on Lithium-Ion Batteries by Solvent Extraction with d2ehpa. *Met. (Basel).* 2021, *11*(1), 54. DOI: 10.3390/met11010054.

[16] Global Manganese Production by Country 2021 | Statista. https://www.statista.com/statistics/1244066/global-manganese-production-volume-by-country/ (accessed March 13, 2024. [Online].

[17] Manganese. https://giyanimetals.com/manganese. (accessed March 13, 2024). [Online].

[18] Cannon, W. F.; Kimball, B. E.; Corathers, L. A. *Critical Mineral Resources of the United States—Economic and Environmental Geology and Prospects for Future Supply*, Reston, Virginia, 2017. DOI: 10.3133/pp1802L.

[19] Sun, X.; Hao, H.; Liu, Z.; Zhao, F. Insights into the Global Flow Pattern of Manganese. *Resour. Policy.* 2020, *65*. DOI: 10.1016/j.resourpol.2019.101578.

[20] Vieceli, N.; Vonderstein, C.; Swiontekc, T.; Stopić, S.; Dertmann, C.; Sojka, R.; Reinhardt, N.; Ekberg, C.; Friedrich, B.; Petranikova, M., et al. Recycling of Li-Ion Batteries from Industrial Processing: Upscaled Hydrometallurgical Treatment and Recovery of High Purity Manganese by Solvent Extraction. *Solvent Extr. Ion Exch.* 2023, *41*(2), 205–220. DOI: 10.1080/07366299.2023.2165405.

[21] Keller, A.; Hlawitschka, M. W.; Bart, H. J. Application of Saponified D2EHPA for the Selective Extraction of Manganese from Spend Lithium-Ion Batteries. *Chem. Eng. Process. - Process Intensif.* Jan, 2022, *171*, 108552. DOI: 10.1016/J.CEP.2021.108552.

[22] Keller, A.; Hlawitschka, M. W.; Bart, H. J. Manganese Recycling of Spent Lithium Ion Batteries via Solvent Extraction. *Sep. Purif. Technol.* 2021, *275*, 119166. DOI: 10.1016/J.SEPPUR.2021.119166.

[23] Peng, C.; Chang, C.; Wang, Z.; Wilson, B. P.; Liu, F.; Lundstro, M. CLEANER MANUFACTURING of CRITICAL METALS Recovery of High-Purity MnO 2 from the Acid Leaching Solution of Spent Li-Ion Batteries. *JOM.* 2020, *72*, 790–799. DOI: 10.1007/s11837-019-03785-1.

[24] Zhang, W.; Cheng, C. Y. Manganese Metallurgy Review. Part II: Manganese Separation and Recovery from Solution. *Hydrometallurgy*. 2007, *89*(3–4), 160–177. DOI: 10.1016/J. HYDROMET.2007.08.009.

[25] Li, J.; Yang, X.; Yin, Z. Recovery of Manganese from Sulfuric Acid Leaching Liquor of Spent Lithium-Ion Batteries and Synthesis of Lithium Ion-Sieve. *J. Environ. Chem. Eng.* 2018, *6*(5), 6407–6413. DOI: 10.1016/J.JECE.2018.09.044.

[26] Malik, M.; Chan, K. H.; Azimi, G. Review on the Synthesis of LiNixmnyco1-X-yO2 (NMC) Cathodes for Lithium-Ion Batteries. *Mater. Today Energy* Aug 1, 2022, *28*. Elsevier Ltd, 10.1016/j.mtener.2022.101066.

[27] Rydberg, J.; Cox, M.; Musikas, C.; Choppin, G. R. Solvent Extraction Principles and Practice, Revised and Expanded, 2004. DOI: 10.1201/9780203021460.

[28] Jantunen, N.; Kauppinen, T.; Salminen, J.; Virolainen, S.; Lassi, U.; Sainio, T. Separation of Zinc and Iron from Secondary Manganese Sulfate Leachate by Solvent Extraction. *Miner. Eng.* 2021, *173*, 107200. DOI: 10.1016/J.MINENG.2021.107200.

[29] Vieceli, N.; Ottink, T.; Stopic, S.; Dertmann, C.; Swiontek, T.; Vonderstein, C.; Sojka, R.; Reinhardt, N.; Ekberg, C.; Friedrich, B., et al. Solvent Extraction of Cobalt from Spent Lithium-Ion Batteries: Dynamic Optimization of the Number of Extraction Stages Using Factorial Design of Experiments and Response Surface Methodology. *Sep. Purif. Technol.* 2023, *307*(November 2022), 122793. DOI: 10.1016/j.seppur.2022.122793.

[30] Cheng, C. Y. Purification of Synthetic Laterite Leach Solution by Solvent Extraction Using D2EHPA. *Hydrometallurgy*. 2000, *56*(3), 369–386. DOI: 10.1016/S0304-386X(00) 00095-5.

[31] Grymonprez, B.; Lommelen, R.; Bussé, J.; Binnemans, K.; Riaño, S. Solubility of di-(2-ethylhexyl)phosphoric acid (D2EHPA) in aqueous electrolyte solutions: Studies relevant to liquid-liquid extraction. *Sep. Purif. Technol.* 2024, *333*, 125846. DOI: 10.1016/ J.SEPPUR.2023.125846.

[32] Lee, P. C.; Li, C. W.; Chen, J. Y.; Li, Y. S.; Chen, S. S. Dissolution of D2EHPA in Liquid-Liquid Extraction Process: Implication on Metal Removal and Organic Content of the Treated Water. *Water Res.* 2011, *45*(18), 5953–5958. DOI: 10.1016/j.watres.2011. 08.054.

[33] Schmitt, J. M.; Blake, C. A., Jr. *Purification of Di(2-Ethylhexyl)phosphoric Acid*, 26th ed.; Oak Ridge: Tennessee, 1964.

[34] Nasser, O. A.; Petranikova, M. Review of Achieved Purities After Li-Ion Batteries Hydrometallurgical Treatment and Impurities Effects on the Cathode Performance. *Batteries*. 2021, *7*(3). DOI: 10.3390/batteries7030060.

[35] Chen, M.; Zhao, E.; Chen, D.; Wu, M.; Han, S.; Huang, Q.; Yang, L.; Xiao, X.; Hu, Z. Decreasing Li/Ni Disorder and Improving the Electrochemical Performances of Ni-Rich LiNi0.8co0.1mn0.1o2 by Ca Doping. *Inorg. Chem.* 2017, *56*(14), 8355–8362. DOI: 10.1021/ACS.INORGCHEM.7B01035/ASSET/IMAGES/LARGE/ IC-2017-010356_0006.JPEG.

[36] Zhang, R.; Zheng, Y.; Yao, Z.; Vanaphuti, P.; Ma, X.; Bong, S.; Chen, M.; Liu, Y.; Cheng, F.; Yang, Z., et al. Systematic Study of Al Impurity for NCM622 Cathode Materials. *ACS Sustain. Chem. Eng.* 2020, *8*(26), 9875–9884. DOI: 10.1021/ ACSSUSCHEMENG.0C02965/ASSET/IMAGES/LARGE/SC0C02965_0005.JPEG.

[37] Wu, T.; Wang, G.; Liu, B.; Huang, Q.; Su, Y.; Wu, F.; Kelly, R. M. The Role of Cu Impurity on the Structure and Electrochemical Performance of Ni-Rich Cathode Material for Lithium-Ion Batteries. *J. Power Sour.* 2021, *494*, 229774. DOI: 10.1016/j. jpowsour.2021.229774.

[38] Park, S. The Effect of Fe as an Impurity Element for Sustainable Resynthesis of Li[ni1/3Co1/3Mn1/3]O2 Cathode Material from Spent Lithium-Ion Batteries. *Electrochim. Acta.* 2019, *296*, 814–822. DOI: 10.1016/j.electacta.2018.11.001.

[39] Di-(2-Ethylhexyl)phosphoric Acid | C16H35O4P | ChemSpider. http://www.chemspider.com/Chemical-Structure.8918.html. (accessed March 17, 2024). [Online].

[40] Mono-(2-Ethylhexyl)-Phosphoric Acid CAS#: 14660-16-3. https://www.chemicalbook.com/ProductChemicalPropertiesCB14634437_EN.htm. (accessed March 17, 2024). [Online].

[41] Tris(2-Ethylhexyl) Phosphate | 78-42-2. https://www.chemicalbook.com/ChemicalProductProperty_EN_CB4670674.htm. (accessed Mar 17, 2024). [Online].

[42] 2-ETHYL HEXANOL | CAMEO Chemicals | NOAA. https://cameochemicals.noaa.gov/chemical/8639. (accessed March 17, 2024). [Online].